

# X-linked retinoschisis: OCT-angiography in two brothers from a four-generation family with a p.Arg197Cys pathogenic variant in the *RS1* gene

European Journal of Ophthalmology  
2023, Vol. 33(5) NP109–NP114  
© The Author(s) 2022  
Article reuse guidelines:  
sagepub.com/journals-permissions  
DOI: 10.1177/11206721221136315  
journals.sagepub.com/home/ejo



Arturo Carta<sup>1</sup> , Roberta Farci<sup>2</sup>, Maria Silvana Galantuomo<sup>2</sup>  
and Maurizio Fossarello<sup>2</sup> 

## Abstract

**Introduction:** X-linked juvenile retinoschisis (XLRS) is a rare genetic disease causing retinal splitting. The aim of this work is to describe the optical coherence tomography angiography (OCTA) features in two brothers affected by an hemizygous c.589C>T (p.Arg197Cys) pathogenic variant in exon 6 of the *RS1* gene.

**Case description:** Each patient underwent a complete ophthalmological examination, including measurement of best corrected visual acuity, slit-lamp biomicroscopy, fundus color photographs, fundus autofluorescence and infrared imaging, fluorescein angiography, spectral-domain optical coherence tomography (SD-OCT) and optical coherence tomography angiography (OCTA). En Face SD-OCT and OCTA revealed the presence of two different pattern of cystic lesions, fusiform and oval, disposed on a petaloid or irregular manner in the perifoveolar area. A widening of the foveal avascular zone with interruption of the vascular arcades was clearly evident. Furthermore, a capillary drop-out was observed in the superficial plexus of the central retina, other than capillary ectasia in the deep capillary plexus. Straight gray lines were visible among the cysts.

**Conclusions:** OCTA data herein described allow a detailed morphological evaluation of XLRS other than a quantitative assessment of retinal capillary flow in this disease. The retinal alterations that we have reported may be helpful to better understand this rare condition with OCTA being a sensitive technique to monitor the evolution of the disease and the response to potential future therapeutic approaches aimed to restore vision.

## Keywords

OCT-angiography, x-linked juvenile retinoschisis, hereditary macular degeneration, retinal inherited rare disease, retinoschisis, macular cysts.

Date received: 10 March 2022; accepted: 24 September 2022

## Introduction

X-linked juvenile retinoschisis (XLRS) is a rare hereditary vitreoretinal dystrophy characterized by symmetric bilateral foveal schisis associated with low visual acuity that begins in the first decade of life, with a prevalence of 1/5000 to 1/25,000 depending on series.<sup>1</sup> It is transmitted as a X-linked recessive trait, affecting almost exclusively male subjects whereas heterozygous females rarely manifest the complete pathologic phenotype. XLRS penetrance is almost complete, but its expression is clinically highly variable. In the vast majority of cases the underlying

cause can be identified in pathogenic variants expression of the retinoschisin 1 gene (*RS1* OMIM: 312700) which is located on the short arm of the X-chromosome

<sup>1</sup>Ophthalmology Unit, Department of Medicine and Surgery, University of Parma, Parma, Italy

<sup>2</sup>Eye Clinic, University of Cagliari, Cagliari, Italy

### Corresponding author:

Arturo Carta, Ophthalmology Unit, Department of Medicine and Surgery, University of Parma, Parma, Italy.

Email: arturo.carta@unipr.it

(Xp22.13). This gene encodes a protein called retinoschisin, a 224 amino acid protein secreted from photoreceptors and bipolar cells, whose function is supposed to guarantee the development and maintenance of the retina, retinal structural integrity, and the post synaptic transmission of photoreceptor signal.<sup>2</sup>

Fundus examination reveals foveal schisis cavities in the nerve fiber layer, giving the impression of a spoke-wheel pattern at macular level. An involvement of outer retinal layers has been also reported in almost 50% of the patients and schisis may be found also in the temporal retinal periphery, predominantly in the inferior temporal quadrant. Usually, macular retinal pigment epithelial irregularities and atrophy are observed in late stages.<sup>3,4</sup> Less common complications foresee vascular changes, including peripheral dendritic vessels, angioma, and vaso-proliferative tumor have been reported with very uncommon complications being represented by vitreous hemorrhage, macular hole, foveal ectopia, retinal detachment with epiretinal membrane, and neovascular glaucoma. The most common refractive error associated to XLRS is mild hyperopia and best corrected visual acuity (BCVA) is usually symmetrically reduced between 0.1 and 0.6 Log MAR; this further deteriorates during the first and second decades of life and may drop to 20/200 in the elderly due to late macular atrophy.<sup>5</sup>

Full-field electroretinography (ERG) represents an important diagnostic tool. Typically, the ERG shows negative-shaped responses (normal a wave, reduced b-wave, with b/a ratio <1), revealing the inner retinal cell dysfunction.<sup>6</sup>

The use of topical and/or systemic carbonic anhydrase inhibitors may help in reducing macular cystic spaces and retinal thickness with a concomitant increase in visual acuity.<sup>7,8</sup>

OCTA is a relatively new imaging technique that permits the detection of retinal and choroidal vessels by mean of split-spectrum amplitude-decorrelation angiography and/or an “en face” OCT-derived technique without any dye injection. In general, the vascular structures observable are as following: the superficial capillary plexus (SCP), the deep retinal capillary plexus (DCP), the choroidal capillary layer (CCL), plus one normally avascular layer, the outer retinal layer (ORL), corresponding to retinal pigment epithelium (RPE)–Bruch’s membrane complex. The segmentation of the vascular layers at various depths allows a detailed analysis of their morphology and capillary flow density (CFD), visible as a color grade scale. A study of small series of OCTA in XLRS reported perifoveal telangiectasias, interruption of the capillary network, enlarged, or irregular, or lack of an appreciable FAZ, and flow loss within the SCP and DCP.<sup>9, 10</sup>

The aim of this work was to describe the clinical phenotype of two siblings affected by XLRS associated with an hemizygous c.589C>T (p.Arg197Cys) pathogenic variant

in exon 6 of the *RS1* gene; we have further analyzed the retinal vascular pattern alterations and the capillary flow density maps as detected by OCTA.

## Case description

The 2 cases herein reported were evaluated at the Eye Clinic of the University of Cagliari; ethical approval for retrospective analysis of their data was granted by the Institutional Review Board of the University of Cagliari, and the study adhered to the tenets of the Declaration of Helsinki. Genotypic and phenotypic characterization of the two siblings has been reported in a previous work.<sup>11</sup> Briefly, individuals from a four-generation family with *RS1* related retinoschisis were recruited at Buddusò which is small village of less than 4000 people in the northern part of the island of Sardinia in Italy. The family consisted of 20 members with four affected subjects (Figure 1). Eleven individuals, including two siblings with *RS1* related retinoschisis (patients 1 and 2 in this paper), underwent a full medical history examination and a comprehensive ocular assessment, electrophysiology and genetic analysis. Sequence analysis of the *RS1* gene identified a hemizygous c.589C>T (p.Arg197Cys) pathogenic variant in exon 6 in the two siblings, hemizygous for this abnormality.

All the family members were yearly evaluated in our clinic with particular attention to the two affected siblings. At the last annual visit they were extensively re-evaluated with a comprehensive ophthalmological examination, including measurement of BCVA, slit-lamp biomicroscopy, fundus color photographs, fundus autofluorescence and infrared imaging, fluorescein angiography (Topcon Engineering, USA), spectral-domain optical coherence tomography (SD-OCT) (Cirrus 4000, Carl Zeiss Meditec, Germany) and optical coherence tomography angiography (OCTA) (AngioVue, RTVue XR Avanti, Optovue, Inc., Fremont, CA). OCTA analysis included descriptive statistics (using Microsoft Office Excel; version 14.0, 2010, Redmond, WA) for qualitative description of imaging characteristics.

## Case I

This is the case of a 27-year-old man, with BCVA of 20/40 in the right eye and 20/32 in the left eye; his refraction was +1.00 of spherical equivalent in both eyes with an axial length of 21.65 mm on the right eye and 21.72 mm in his left eye.

Slight lamp examination of the anterior ocular segment was normal. Dilated fundus examination showed subtle foveal changes. SD-OCT revealed bilaterally a broad intraretinal hyporeflective space extending from inner limiting membrane to photoreceptor layer, associated with smaller cysts in correspondence of the outer nuclear layer

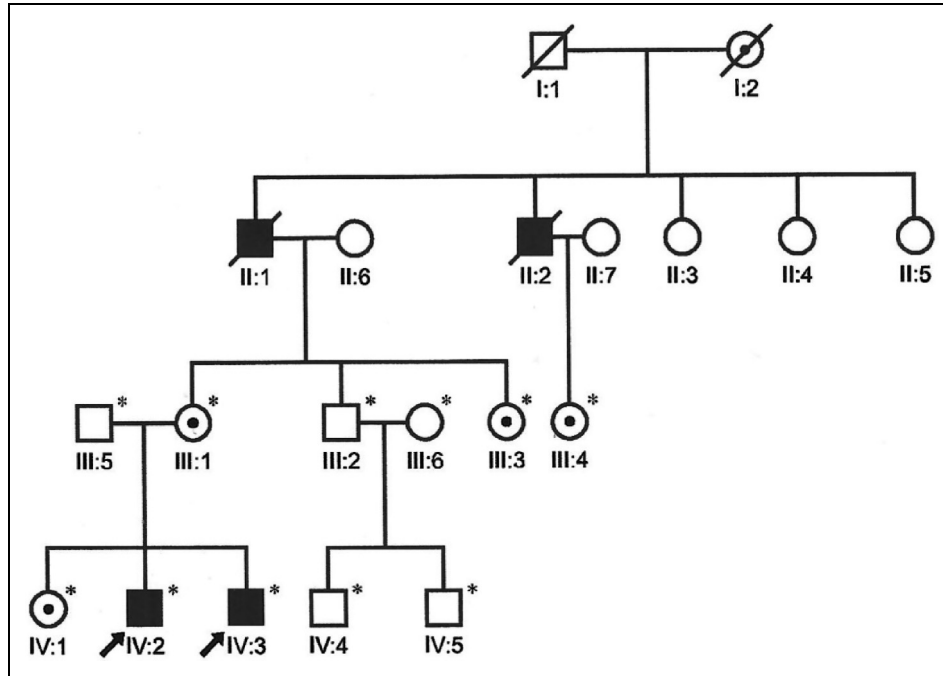


**Figure 1.** The pedigree tree of the four generation family examined by our staff. Unaffected members are represented by empty symbols. Solid squares denote affected males with those crossed by a line meaning that they are dead at the time of the present re-evaluation. Females carriers are indicated by a shade dot inside the circle. Each generation is identified by a Roman number and each individual within the same generation is numbered consecutively by an Arabic number. The patients described in this case report are indicated by a dark arrow.

and of the ganglion cells layer (Figure 2(a) to (h)). Fluorescein angiography highlighted no early or late leakage, typical of macular cystic spaces. Electroretinogram (ERG) examination was similar in both cases herein reported, showing a significantly reduced rod and cone responses for the amplitude of the *a*- and *b*-waves.

OCTA showed an enlargement of the avascular foveal zone in correspondence of SCP, with a complete interruption of the foveal arcade in inferior temporal quadrant of right eye and in superior-temporal and inferior-nasal sector of left eye. Optovue XR Avanti flow tool confirmed the absence of capillary perfusion around the fovea. In the deep capillary plexus decorrelation signal was augmented 360° around near the schisis, as confirmed by Capillary Density Flow analysis (Figure 3). Schisis spaces were easily detectable also on En Face OCT images.

## Case 2

This is the case of a 25-year-old man (sibling of patient 1) which showed a BCVA of 20/32 bilaterally with a +2.00 of spherical equivalent and an axial length of 21.21 and 21.56 mm respectively for the right and for his left eye. Slight lamp examination of the anterior segment was within normal limits but on funduscopy subtle foveal changes similar to those observed in his sibling were detected in both eyes (Figure 2(i) to (r)).

SD-OCT scans highlighted multiple hyporeflective ovaloid spaces with major vertical diameter, set in foveolar and parafoveolar zone, extending from inner nuclear layer to outer plexiform layer. Microcysts were present in extrafoveal region. Fluorescein angiography revealed hypofluorescent radiate macular spaces, with no leakage and ERG was quite similar to the one described in Case 1.

OCT-A showed FAZ enlargement, with a 360° vascular arcade disruption. Schitic spaces were visible as round or ovaloid hyporeflective regions in correspondence of SCP and DCP, as seen also in En Face OCT. Cystic spaces were less numerous than in patient 1 and CCL did not show pathological alterations (Figure 3).

## Conclusions

In this study, a combined evaluation with SD-OCT and OCTA allows us to individuate bidimensional and tridimensional morphology in XLRs, defining the flow in the superficial and deep capillary plexus around the intraretinal cavities of the two siblings affected.

Patient 1 SD-OCT evaluation showed a spokewheel like pattern of schisis, which was associated with fusiform schisis cavities, whereas patient 2 showed a honeycomb pattern associated with an irregular pattern of round cysts in foveal and iuxta-foveal region. In both patterns, cystic cavities were interspaced by straight gray lines, presumed

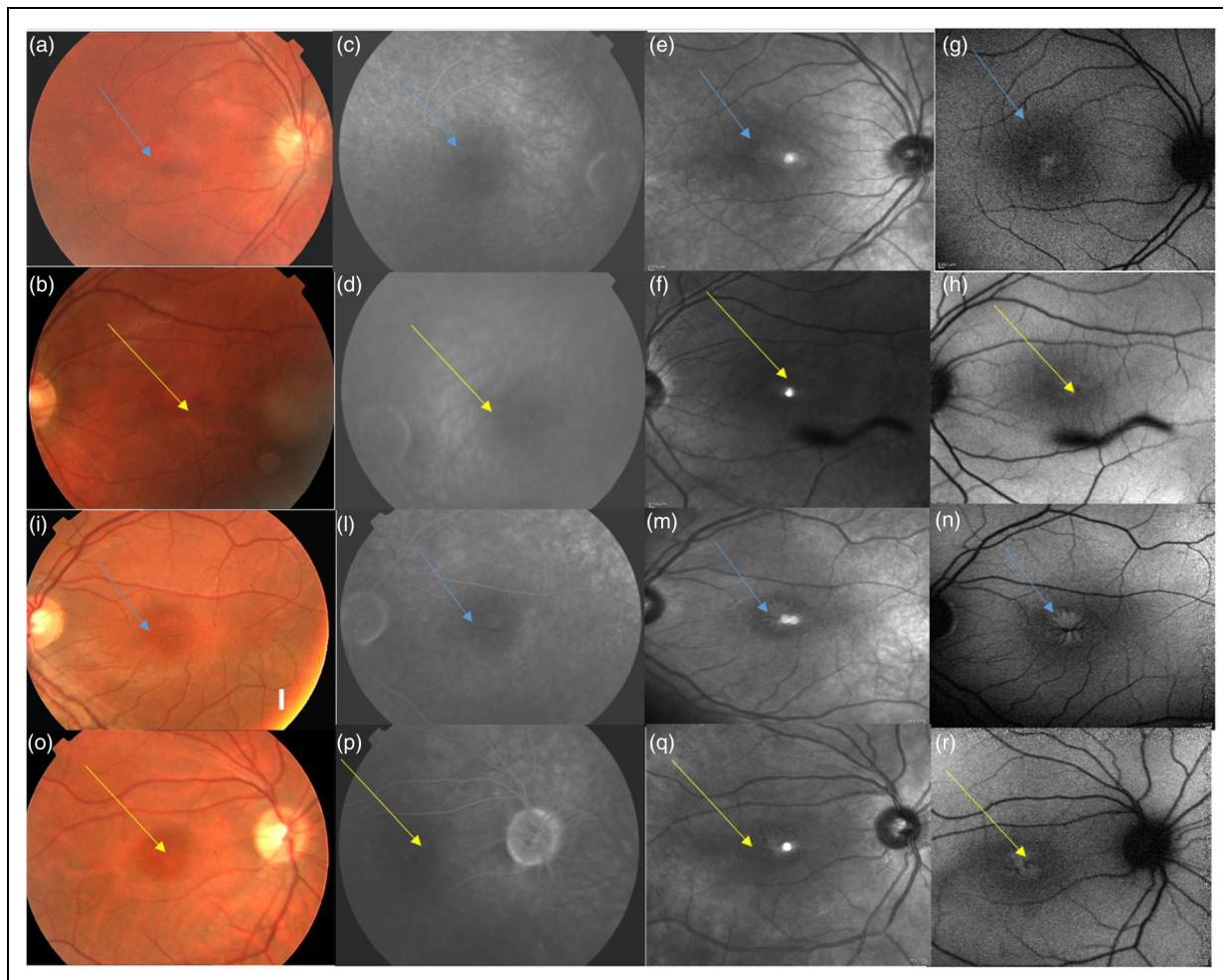


**Figure 2.** (a). Fundus photography shows the absence of foveal reflex (blue arrow). (b) Fluorescein angiography shows the leakage due to cystic spaces (blue arrow). (c) Slo infrared shows schisis as hyporeflective cystic spaces (blue arrow). (d) Autofluorescence shows hyporeflective signal linked to cystic spaces (blue arrow). (e) Fundus photography shows the absence of foveal reflex (yellow arrow). (f) Fluorescein angiography shows the leakage due to cystic spaces (yellow arrow). (g) Slo infrared shows schisis as hyporeflective cystic spaces (yellow arrow). (h) Autofluorescence shows hyporeflective signal linked to cystic spaces (yellow arrow). (i) Fundus photography shows the absence of foveal reflex (blue arrow). (l) Fluorescein angiography shows the leakage due to cystic spaces (blue arrow). (m) Slo infrared shows schisis as hyporeflective cystic spaces (blue arrow). (n) Autofluorescence shows hyporeflective signal linked to cystic spaces (blue arrow). (o) Fundus photography shows the absence of foveal reflex (yellow arrow). (p) Fluorescein angiography shows the leakage due to cystic spaces (yellow arrow). (q) Slo infrared shows schisis as hyporeflective cystic spaces (yellow arrow). (r) Autofluorescence shows hyporeflective signal linked to cystic spaces (yellow arrow).

to be Müller cells axons. Moreover, linear blood vessels were observed surrounding the cystic cavities in petaloid pattern but without telangiectatic vessels, nor aneurysmal dilations.

These different patterns might be explained by variations in the distribution of cells in each retinal layer in the foveal and parafoveal regions, including bipolar, amacrine, horizontal, and Müller cells, as a result of schisis enlargement. In our study, OCTA revealed very similar vascular abnormalities in the two siblings: in the superficial plexus, we observed irregular enlargement of FAZ with vascular arcade interruptions in the SCP, and capillary

dilatation with flow enhancement all around the border of the avascular ovaloid central zone in DCP.

Interestingly, in both cystic patterns OCTA showed capillary drop-out of FAZ only in the SCP, while in DCP areas of flow increment was seen to co-localize with ectatic capillaries at the border of the FAZ. This finding is in accordance to several authors who described microvascular abnormalities in DCP as protrusions of vessels bordering the cystic spaces, probably due to a weakness of the vessel walls secondary to the absence of glial support, or to the hydrostatic force exerted by the cystic liquid content; areas of flow increment appeared

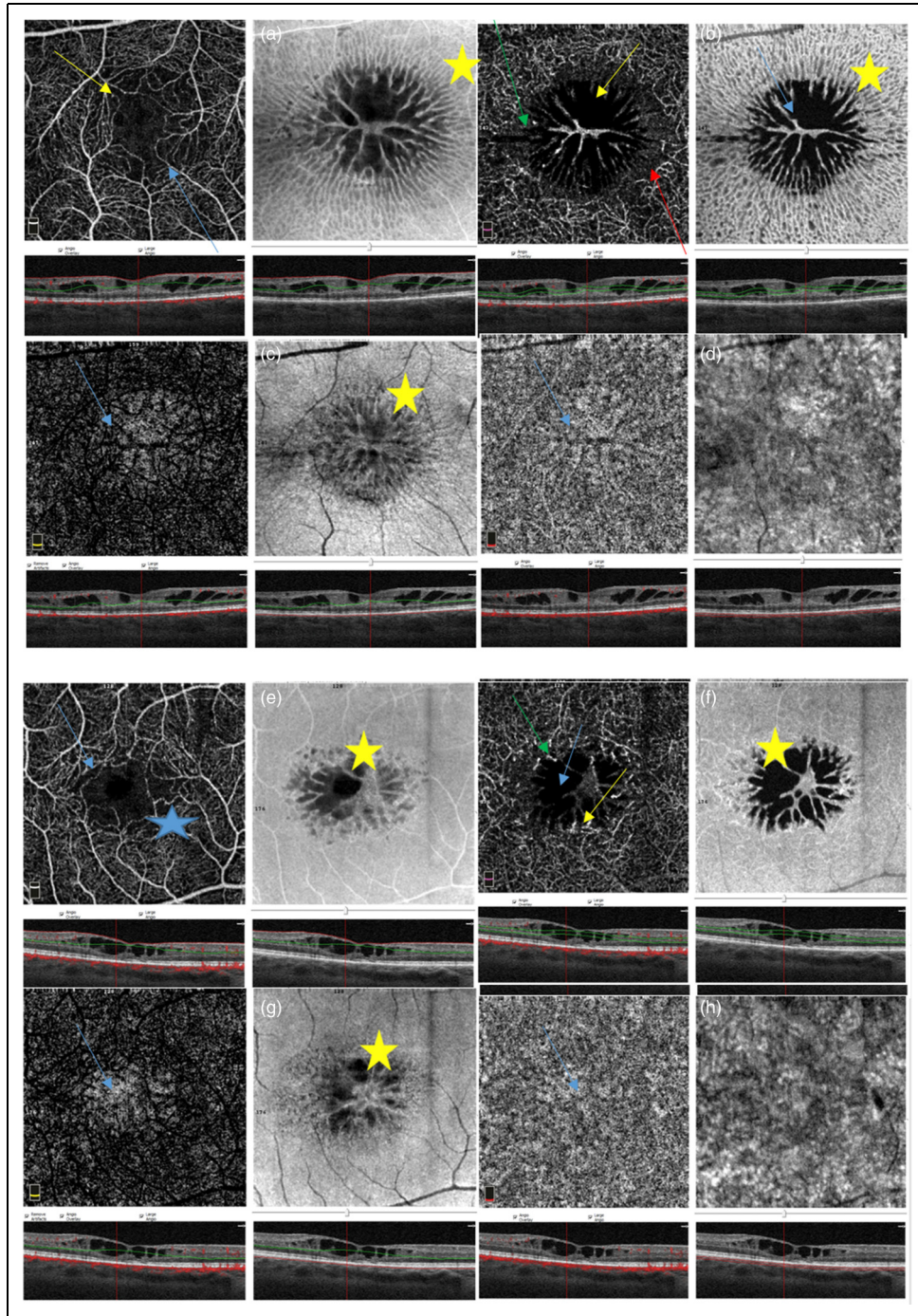


**Figure 3.** Foveal arcade disruption (blue arrow) and capillary network enlarging (yellow arrow) is present in angio OCT superficial capillary Plexus layer. Yellow star indicates cysts at En Face OCT. Angio OCT Deep Capillary Plexus highlights sunbeam shaped disposition of cystic cavities (black fusiform spaces) indicated by the blue arrow, and their walls (yellow arrow), absence of flow signal around cysts (green arrow) and neighboring capillaries ectasies (red arrow); C In outer retinal layer is visible the light causing a decorrelation signal after its passage through the cysts (blue arrow). Yellow star indicates cysts at En Face OCT. D In choroid capillary layer decorrelation signal caused by the light is visible (blue arrow). Yellow star indicates schisis at En Face OCT. E Right eye Angio OCT Superficial Capillary Plexus: blue star shows irregular avascular foveal zone enlargement; blue arrow indicates vascular arcade interruption. Yellow star indicates cysts at En Face OCT. F Right eye Angio OCT Deep Capillary Plexus: cystic space seen as round spaces without decorrelation signal (blue arrow); yellow arrow indicates gray no flow intercystic zone; green arrow indicates capillary dilatation. Yellow star indicates cysts at En Face OCT. G Right eye Angio OCT Outer Retina Layer: blue arrow indicates the artifact due to the passage of the light through cysts. H Right Eye Angio OCT Choroid Capillary Layer (blue star).

interspersed with areas of flow loss and vessels rarefaction where further documented.<sup>9,10,12</sup>

Although photoreceptors and bipolar cells are involved in the disease process, we did not find alterations in correspondence of photoreceptors or choriocapillaris layer. The only authors who described OCTA choriocapillaris changes were Stanga *et al.* and Cennamo *et al.*, who reported hypo and hyper-reflective signals, probably due to the shadow caused by the overlying structures.<sup>9,13</sup>

As regards the schisis content, cystic spaces were visualized with OCTA as uniformly non reflective, optically empty structures, presumably with fluid lacking any motion of particles (i.e., red blood cells, macromolecules, etc.), since a gray appearance would suggest the presence of a liquid content characterized by Brownian movements (i.e., red blood cells, macromolecules, etc.).

As regards the cystic space shape, we realized that in XLRS macular cysts assume a peculiar pattern, which is very different from that observed in cysts associated with macular edema from different etiologies such as diabetes, Branch or Central retinal vein occlusion, or Irvine-Gass post surgical syndrome.

Finally, the most similar aspect to XLRS cysts, is observed in epiretinal membranes due to their tractional effect. In fact, in this tissue schitic lesions are roundish, located within DCP, the content is black, and grey walls are well defined, without any surrounding microvascular or ischemic areas.

In conclusions, XLRS is a leading cause of hereditary juvenile macular degeneration in males resulting in significant vision impairment. Since a wide range of retinal abnormalities has been described in XLRS by different authors, OCTA may be useful in better delineating the clinical phenotype and the vascular alterations of the disease. Furthermore, OCTA may represent a sensitive technique to monitor the evolution of this rare condition other than its response to potential future therapeutic approaches aimed to restore vision.

### Acknowledgements

Sincere thanks to the genetic laboratory of the University of Cagliari.


### Declaration of conflicting interests


The author(s) declared no potential conflicts of interest with respect to the research, authorship, and/or publication of this article.

### Funding

The author(s) received no financial support for the research, authorship, and/or publication of this article

### ORCID iDs

Arturo Carta  <https://orcid.org/0000-0002-6284-0588>

Maurizio Fossarello  <https://orcid.org/0000-0003-1520-7760>

### References

1. Tantri A, Vrabec TR, Cu-Unjieng A, et al. X-linked retinoschisis: a clinical and molecular genetic review. *Surv Ophthalmol* 2004; 49: 214–230.
2. Molday RS, Kellner U and Weber BHF. X-linked juvenile retinoschisis: clinical diagnosis, genetic analysis, and molecular mechanisms. *Prog Retin Eye Res* 2012; 31: 195–212.
3. Gregori NZ, Lam BL, Gregori G, et al. Wide-field spectral-domain optical coherence tomography in patients and carriers of X-linked retinoschisis. *Ophthalmology* 2013; 120: 169–174. doi:10.1016/j.ophtha.2012.07.051
4. Passaro ML, Magno L, Mazzucco A, et al. An unusual association of macular retinoschisis with progressive familial intrahepatic cholestasis: a multimodal imaging study. *Eur J Ophthalmol* 2021. doi:10.1177/11206721211060141
5. Menke MN, Feke GT and Hirose T. Effect of aging on macular features of x-linked retinoschisis assessed with optical coherence tomography. *Retina* 2011; 31: 1186–1192.
6. Bowles K, Cukras C, Turriff A, et al. X-linked retinoschisis: rS1 mutation severity and age affect the ERG phenotype in a cohort of 68 affected male subjects. *Invest Ophthalmol Vis Sci* 2011; 52: 9250–9256. doi:10.1167/iovs.11-8115
7. Andreuzzi P, Fishman GA and Anderson RJ. Use of a carbonic anhydrase inhibitor in X-linked retinoschisis: effect on cystic-appearing macular lesions and visual acuity. *Retina* 2017; 37: 1555–1561. doi:10.1097/IAE.0000000000001379
8. Genead MA, Fishman GA and Walia S. Efficacy of sustained topical dorzolamide therapy for cystic macular lesions in patients with X-linked retinoschisis. *Arch Ophthalmol* 2010; 128: 190–197.
9. Cennamo G, Centore N, Mirra F, et al. Multimodal imaging in retinoschisis X-linked. *Ophthalmol Case Rep* 2018; 2: 8–10.
10. Han IC, Whitmore SS, Critser DB, et al. Wide-Field swept-source OCT and angiography in X-linked retinoschisis. *Ophthalmology Retina* 2019; 3: 178–185. doi:10.1016/j.oret.2018.09.006
11. Galantuomo MS, Fossarello M, Cuccu A, et al. Rebound macular edema following oral Acetazolamide therapy for juvenile X-linked retinoschisis in an Italian family. *Clin Ophthalmol* 2016; 25: 2377–2382.
12. Mastropasqua R, Toto L, Di Antonio L, et al. Optical coherence tomography angiography findings in X-linked retinoschisis. *Ophthalmic Surg Lasers Imaging Retina* 2018; 49: e20–e31. doi:10.3928/23258160-20180907-03
13. Stanga PE, Chong NH, Reck AC, et al. Optical coherence tomography and electrophysiology in X-linked juvenile retinoschisis associated with a novel mutation in the XLRS1 gene. *Retina* 2001; 21: 78–80.